

# Compact Shipboard Antenna System For Simultaneous Communication With Three Separate Satellites

**Dr. E. Walton, Mr. E. Lee, Ms. D. Kohlgraf**

Ohio State Univ. Columbus, OH 614/292-5051

**Mr. R. Pavlovicz, Mr. G. Bruce, Mr. B. Montgomery**

Syntonics Corp. Columbia, MD 410/884-0500

**Abstract - Modern naval ships rely on satellite systems for weather information and communications. For example, the heritage AN/SMQ-11 Shipboard Receiving Terminal for meteorological data provides L- and S-band receive capability with a single flat-panel dual-band antenna array that is pointed at one satellite at a time. Satellite communication (SATCOM) systems require spherical radomes located port and starboard (because of mast blockage) for each frequency band. With limited topside space, locating these multiple radomes is difficult.**

## I. INTRODUCTION

This paper will discuss a new type of satellite communications antenna system where up to three separate satellites can be simultaneously tracked from a single radome. Inside this radome there are up to three nested, mechanically steered, flat plate array antennas. The outer array antennas are transparent to the inner arrays. Modern frequency selective surface (FSS) theory is used in the antenna designs. The positioning system is designed so that the antennas can be independently pointed without colliding with each other. Since the outer antennas are transparent to the inner antennas, when blockage occurs they do not degrade the signals used by the inner antennas.

We will show a new tri-band antenna system design where L-band, S-band, and X-band antennas are nested in the same radome. The flat plate arrays are made using “bow-tie” dipoles for circular polarization. Phase adjustments are made by simply rotating these elements. The elements are located  $1/4$  wavelength above a ground plane, where the ground plane is a FSS array of crossed rods. The transmission line system was a particular challenge, but was designed using thin film stripline technology with thin film directional couplers of variable coupling coefficients.

We will show gain and polarization data on the individual antenna element performance as well as the full array performance. Data on the transmissivity of the FSS ground plane as well as of the full antenna array will be shown. Full performance data on the gain of the antennas in the presence of the outer antennas will also be shown. Final system performance data will be given.

## II. SYSTEM OVERVIEW

### A. Antenna Configuration

A diagram of the antenna configuration is shown in Figure 1. In this figure, it can be seen that the antennas are “nested”. The flat plate array antennas move in a spherical geometry so that they remain broadside to the associated satellite. The outer antennas are designed to be transparent to the inner antennas to avoid blockage effects. As can be seen, the result is a small semi-spherical package with three independently pointing nested antennas.

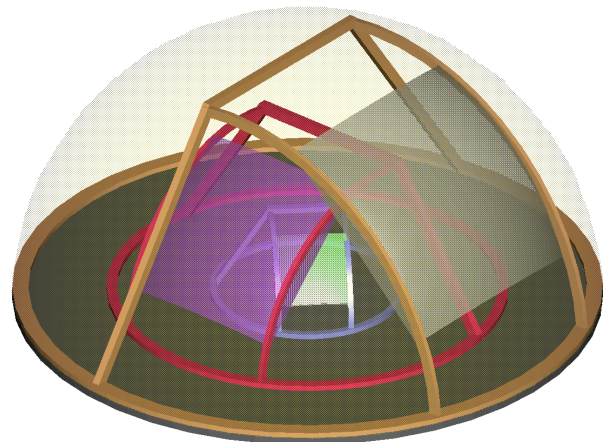


Fig. 1. Overview drawing of nested antennas.

### B. FSS Concepts

The L-band and S-band antenna panels are constructed as an array of relatively narrow circularly polarized radiating elements over a frequency selective surface (FSS) ground plane. (The inner X-band array is a standard flat panel array.) The theory of FSS arrays is given in [1]. The initial design was modeled using a periodic moment method code [2] developed at The Ohio State University (OSU). In this case, a “+” shaped conducting element interleaved with an “x” shaped element is used so that the FSS will be relatively narrow band. It will be a reflective ground plane over its operational band and transparent over other frequency bands. A diagram of the FSS layer is

shown in fig. 2.

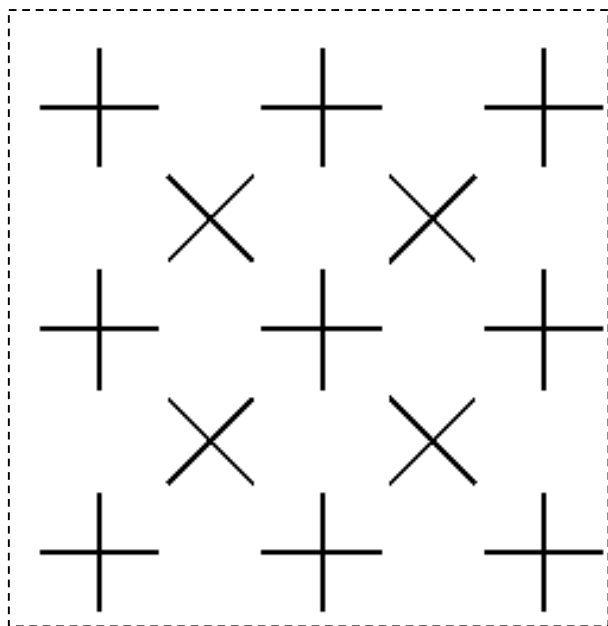


Fig. 2. Example FSS layer

Note that the FSS elements are relatively far apart to reduce capacitive coupling which would increase the bandwidth.

### C. CP element

The CP element used in the design uses a basic crossed dipole/loop shape as shown in Fig. 3, but with a small gap in one of the arms to shift the phase to give circular polarization [2]. This element reduces the complexity of the feed network because it can be fed at the center in the same way as a simple dipole. Tests show that 7 to 8 dBiC gain is achieved with good CP performance over our desired band. This relatively high gain permits larger element spacing and fewer elements because the grating lobes are not excited even at a spacing of nearly 1 wavelength.

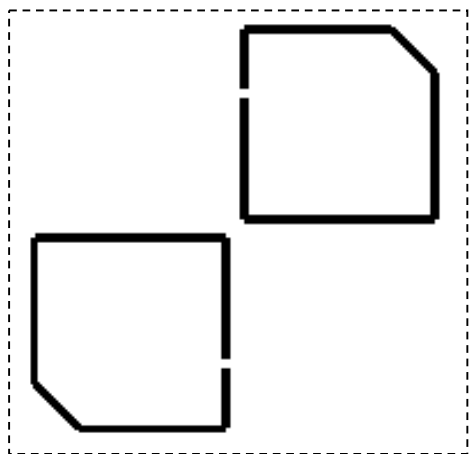


Fig. 3. Circularly polarized radiating element

### D. Array geometry

The L-band array is basically a 12x12 element array while the S-band array is basically a 14x14 array. The corners are truncated so that the final shape is approximately hexagonal. An example drawing of one of the L-band array layouts under consideration is shown in figure 4.

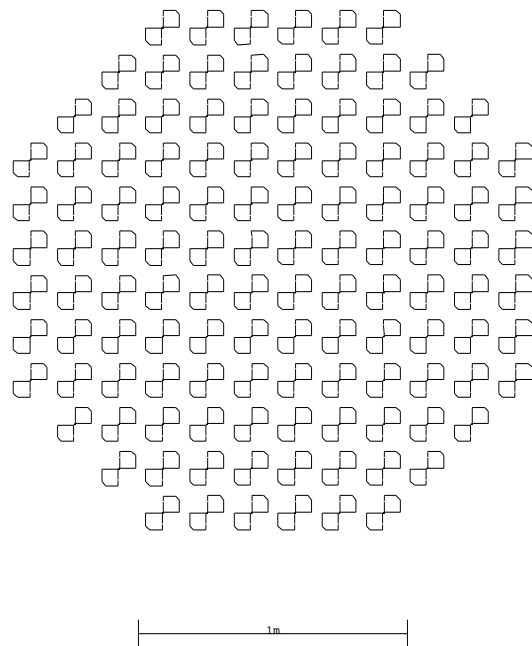


Fig. 4. Example drawing of the L-band array layout showing radiating elements without FSS ground plane.

### E. Transmission Lines

The transmission lines are located in a layer behind the FSS ground plane. These transmission lines are designed to minimize the amount of blockage that they present. This is done by using a variable power coupling distributed Hybrid coupler design. In this design, the array is divided into 4 quadrants, and the feed structure provides an adjusted power coupling at each point so that the final design provides the same power to each of the radiating elements. The basic layout of the transmission line system is shown in figure 5.

Note the 4 quadrants, each with a main branch and a set of side branches. It can be seen that the power division must be carefully computed to achieve equal power delivered to the individual elements. The four quadrant design permits monopulse tracking of the received signals.

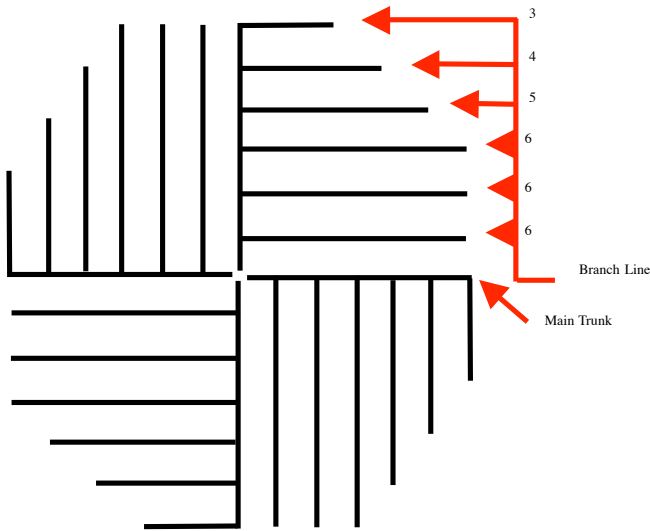


Fig. 5. Basic transmission line layout.

The transmission lines are designed as balanced lines. They are printed lines on both sides of a thin layer of dielectric so that the blockage is minimized. The connection from the transmission line layer to the radiating element layer is just a turn in the coupled lines to provide coupling between the radiating elements and the transmission line layer. Note that this design (as compared to a corporate feed system) results in a non-equal distribution of phase to the feed points. This is compensated for by simply twisting the transmission line in a spiral so that the circularly polarized (CP) radiating elements can be rotated to shift the phase. The final layout will have the CP elements oriented so that the radiated CP signals are all in-phase.

#### F. Final panel lay-up

The final lay-up for the L-band and the S-band flat

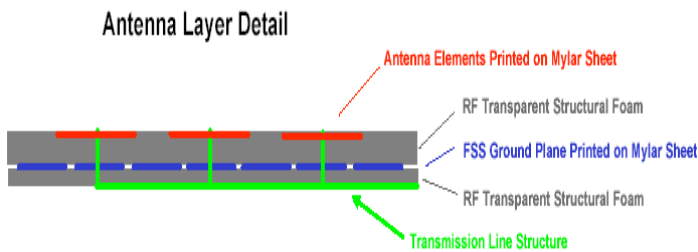


Fig. 6. Final panel lay-up (note the radiating elements, the FSS ground plane, and the transmission line layers).

Note the radiating elements on top (copper/silver printed on Mylar, the Styrofoam inner core, the FSS ground plane (also printed on Mylar), and the transmission lines (copper printed on dielectric). The final panel is very light weight and low cost. The Mylar skins on the Styrofoam inner core give a strong and rigid final

structure. The adhesive must be low loss.

### III. MODELING

#### A. ESP5 Model

The entire structure with both L-band and S-band arrays, including the radiating elements, the FSS ground planes, and the transmission lines has been modeled using a wire-grid method of moment (MOM) code developed at OSU [3]. The final model used many hundreds of wire elements. Both the gain pattern and the transmissivity of the arrays were modeled. The MOM model is very robust, although the code takes 3 to 6 hours to run on a large sized Pentium IV machine. (Most of the runs are done overnight.)

#### B. Theoretical Modeling Results

The gain pattern of the hexagonal 12x12 L-band array is shown in figure 7. Also shown on this figure are the desired gain levels and the desired side lobe levels. Note that the gain pattern of the array meets all of these requirements.

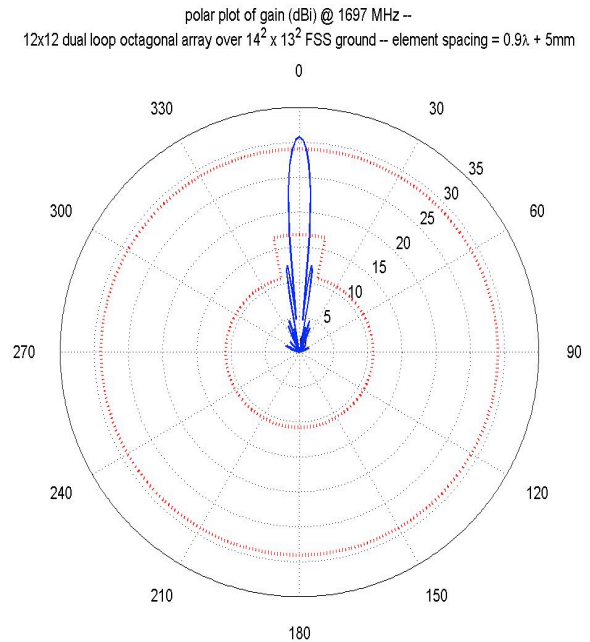


Fig. 7. Gain pattern of the L-band hexagonal array. (note the outer red dotted curve (gain requirement) and the inner red dotted curve (sidelobe requirements))

An MOM model of the transmissivity of an 8x8 element L-band array antenna as seen by an 8x8 version of the S-band array was created. The results of a transmissivity study are shown in Figure 8. In this case, the S-band array is “looking through” the L-band array at various offsets and angles. Note that the reference line is the boresite signal with no array blockage. The other lines show blockage effects as a function of frequency for

various relative pointing angles and blockage coverage. Note the dip in transmissivity at the operational frequency of the FSS ground plane. This is the operational frequency of the L-band array where the FSS must serve as a ground plane. Note that the transmissivity of the L-band antenna approaches the reference case (no antenna) for frequencies above 2.2 GHz. (Oscillations above and below this value are standing wave effects in the model.)

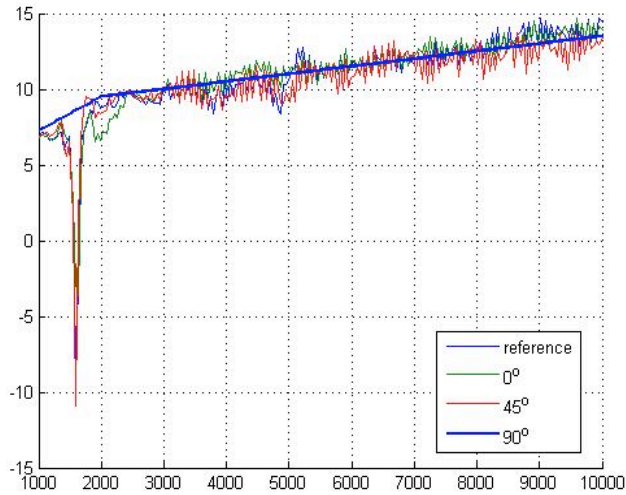


Fig. 8. Transmissivity Study for 8x8 S-band array looking through 8x8 L-band array.

### C. Experimental Testing Results

A sub-scale (4 x 1) array with a FSS ground plane was built and the gain pattern and transmissivity were measured as a preliminary test. The gain pattern of the

array was as predicted by the theory, and the transmissivity was within expectations.

### IV. CONCLUSIONS

The three antenna structure is presently under construction. When completed, it will be possible to have three antennas operating independently in a single radome occupying the space normally needed for each of the three antennas. A sketch of the support/positioning structure is shown in Figure . The weight of the mostly Styrofoam structures will be very low. The cost will be low because the materials are only Styrofoam panels and copper patterns printed on Mylar or a dielectric. New data on the performance of the overall structure will be available in early 2006.

### REFERENCES

[1] Ben A. Munk, *Frequency Selective Surfaces: Theory and Design*, (New York: John Wiley & Sons, Inc., 2000.)  
 [2] L. W. Henderson, "Introduction to PMM, Version 4.0," The Ohio State Univ., EletroScience Lab., Columbus, OH, Tech. Rep. 725 347-1, Contract SC-SP18-91-0001, Jul. 1993.  
 [3] E. H. Newman, *A User's Manual for The Electromagnetic Surface Patch Code: Release Version ESP5.3*, The Ohio State Univ., EletroScience Lab., Columbus, OH, 2004.  
 [4] H. Morshita, K. Hirasawa, T. Nagao, "Circularly polarized wire antenna with a dual rhombic loop", IEEE Proc-Microwave Antennas Propag., vol. 145, pp. 219-224, 1998.

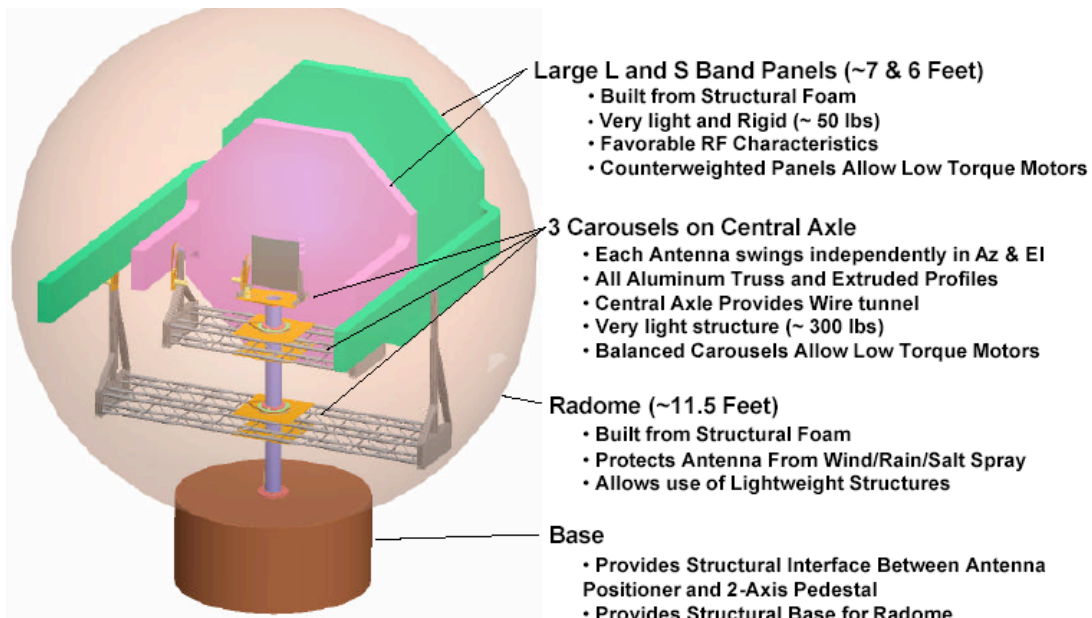


Fig. 9. Overall layout of the three antennas on a positioning structure in a radome.